

1. Introduction

- The Stepped-Frequency Microwave Radiometer (SFMR) obtains surface wind speed measurements in tropical cyclones (Figure 1).

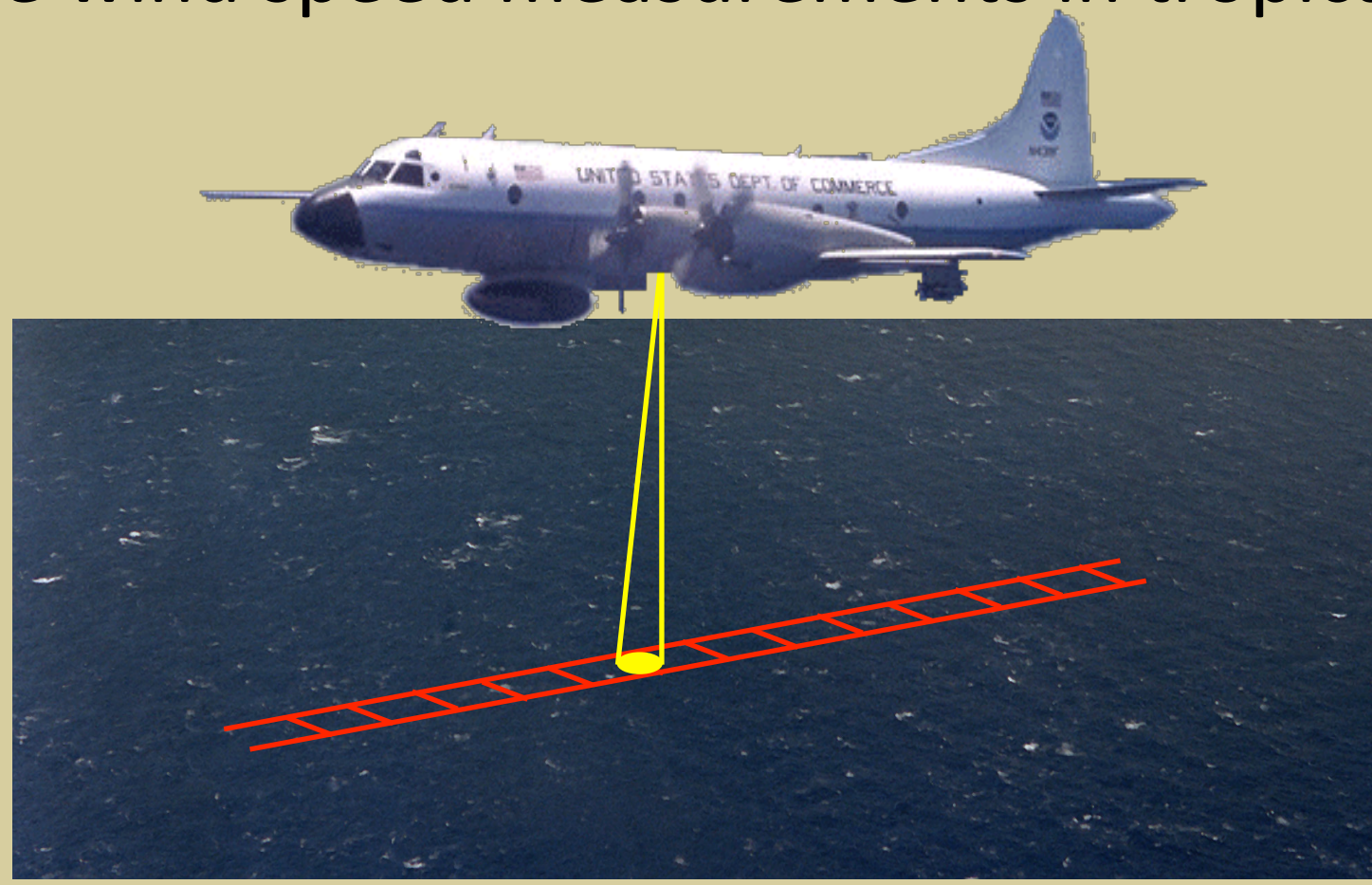


Figure 1: Schematic depicting the SFMR footprint (yellow) and nadir track (red).

- Due to poor knowledge about sea surface microwave emission at large Earth incidence angles (EIA) and high wind speeds, SFMR wind speeds are only retrieved at nadir incidence beneath the aircraft.
- Understanding the relationship between the SFMR measured brightness temperatures (T_B), which are used to obtain a surface wind speed, and the ocean surface wave field at off-nadir EIA would potentially allow for the retrieval of wind speeds at off-nadir EIA.
 - Improving the probability of measuring the peak wind speed.
- It is hypothesized that at off-nadir EIA, the distribution of foam on the ocean surface from breaking waves impacts the SFMR measurements differently than at nadir.
- Analysis of excess T_B (ΔT_B) measured in Hurricane Gustav (2008) at 30° and 45° incidence indicate the presence of a double-harmonic oscillation, which may be due to variations in wind or wave directions.

2. SFMR



Figure 2: Picture of the SFMR wing pod installed on the aircraft and the SFMR instrument itself. (image source: www.prosensing.com)

- SFMR is a C-band microwave radiometer that measures radiative emissions, primarily from foam on the sea surface, at six frequencies, 4.74, 5.31, 5.57, 6.02, 6.69, and 7.09 GHz to estimate the surface wind speed and rainfall rate (Uhlhorn et al. 2007).
- A forward radiative transfer model is used to estimate the T_B of the sea surface for each of the frequencies (Uhlhorn and Black 2003).
- Spatial resolution of 1.5 km along the flight track with a cross-track footprint diameter of between 600 and 800 m at a typical flight altitude of 1500 m (Uhlhorn and Black 2003).
- Flown on NOAA WP-3D aircraft and Air Force Reserve Command WC-130J aircraft and is installed within a pod underneath the aircraft's wing (Figure 2).

3. Hurricane Gustav (2008)

- A SFMR module was flown in Hurricane Gustav to retrieve surface T_B measurements at off-nadir EIA.
- Gustav (Figure 3) was a category 3 storm at the time of the flight with estimated peak winds of 51 m/s.
- The module consisted of four circles, one flown at an aircraft roll angle of 30° followed by three at an aircraft roll angle of 45°, in a rain-free portion of the eyewall (Figure 4) where the surface wind speed measured by a GPS dropwindsonde was 35 m/s.

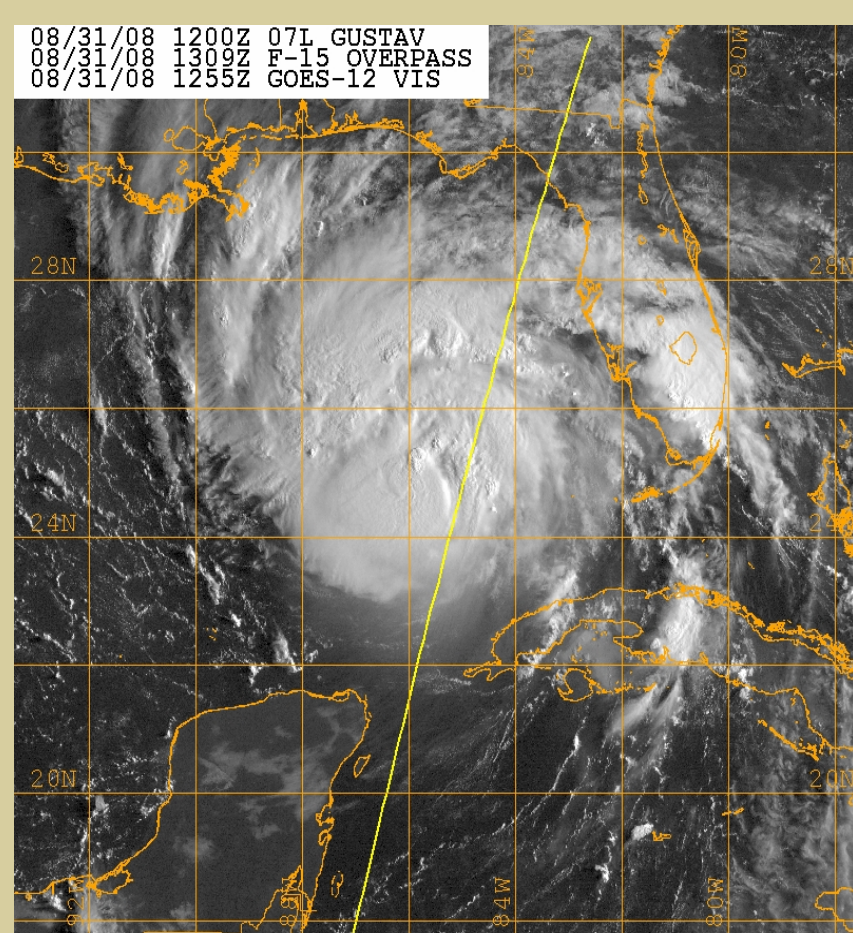


Figure 3: Visible imagery of Hurricane Gustav on August 31, 2008 (image source: www.aoml.noaa.gov/hrd).

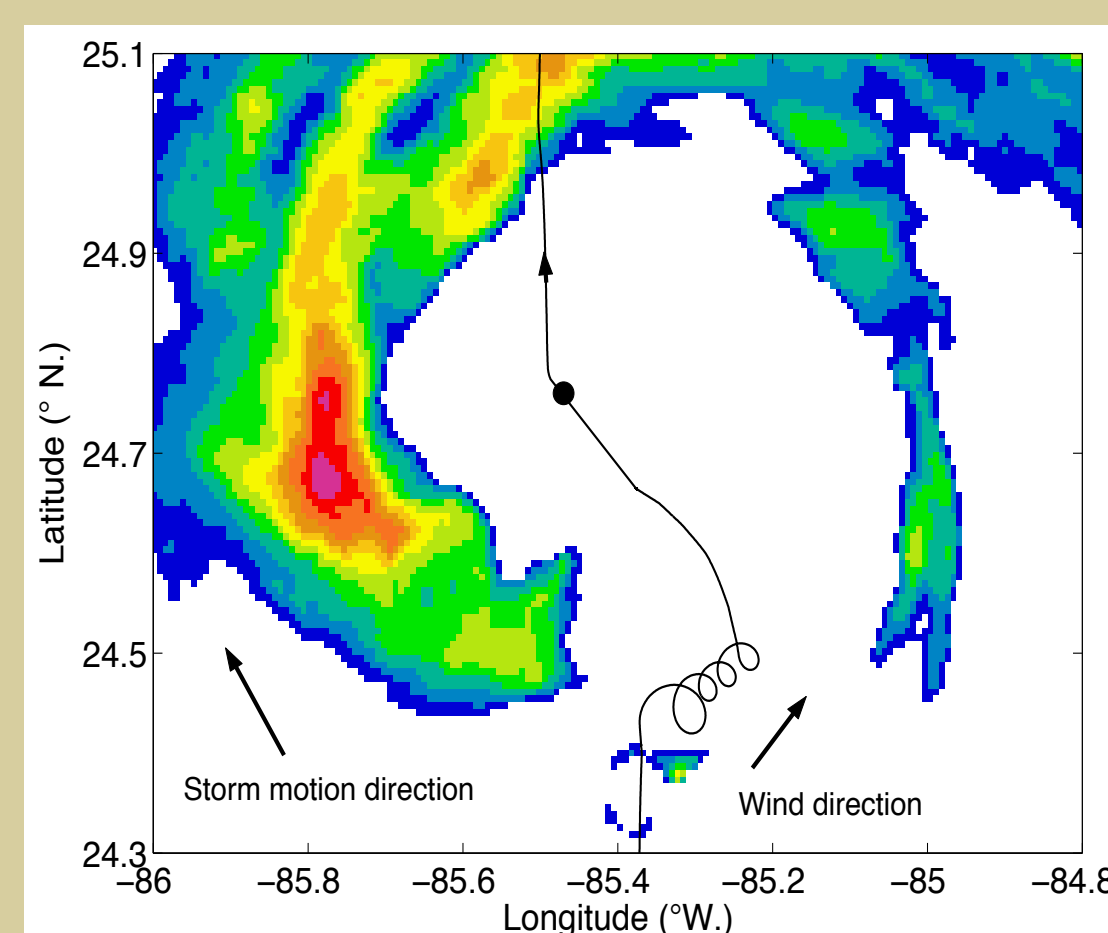


Figure 4: NOAA P-3 aircraft lower-fuselage radar reflectivity for Hurricane Gustav on August 31, 2008 with the flight track.

8. References

- Gaiser et al., 2004: The WindSat spaceborne polarimetric radiometer: Sensor description and early orbit performance. *IEEE Trans. Geosci. Remote Sensing*, **42**, 2347–2361.
- Klein, L.A., and C.A. Swift, 1977: An improved model for the dielectric constant of sea water at microwave frequencies. *IEEE J. Oceanic Eng.*, **OE-2**, 104–111.
- Kunkee, D.B., and A.J. Gasiewski, 1997: Simulation of passive microwave wind direction signatures over the ocean using an asymmetric-wave geometrical optics model. *Radio Sci.*, **32**, 59–78.
- Tolman, H. L., 2002: User manual and system documentation of WAVEWATCH-III version 2.22. *NOAA/NWS/NCEP/OMB technical note.*, **222**, 133 pp.
- Uhlhorn et al., 2007: Hurricane surface wind measurements from an operational Stepped-Frequency Microwave Radiometer. *Mon. Wea. Rev.*, **135**, 3070–3085.
- Uhlhorn, E.W., and P.G. Black, 2003: Verification of remotely sensed sea surface winds in hurricanes. *J. Atmos. Oceanic Technol.*, **20**, 99–116.

4. Measurements From Gustav

- SFMR and flight level data from Gustav are shown in Figure 5.
- ΔT_B is calculated for the SFMR T_B measured in Hurricane Gustav by subtracting the expected zero wind speed T_B (calculated using the Klein and Swift (1977) algorithm).
- The ΔT_B are then detrended and fit with a Fourier series using least-squares regression (Figure 6):

$$\Delta T_B = \sum_{n=0}^3 A_n \cos n(\theta_r + \phi_n)$$
 - A_n and ϕ_n are fitted parameters corresponding to the n -th harmonic amplitudes and phase angles, respectively.
- The ΔT_B are expressed as a function of wind direction minus relative azimuth angle (aircraft heading minus 90°), which is referred to as the relative look angle (θ_r).

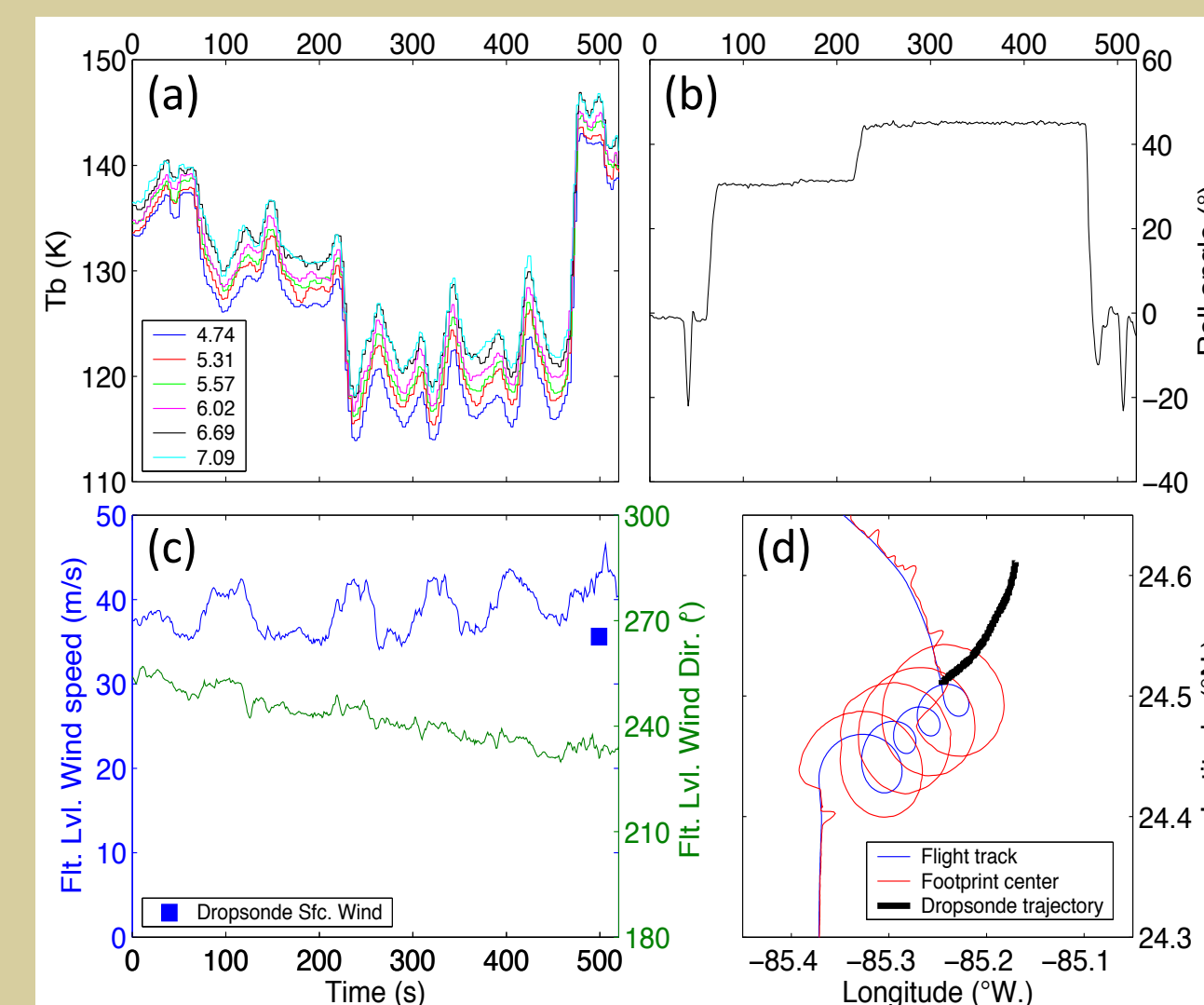


Figure 5: Time series of SFMR T_B (a), roll angle (b), flight-level wind speed and direction (c), and flight track (d). Also shown in (c) is the surface (10-m) GPS dropwindsonde measured wind speed.

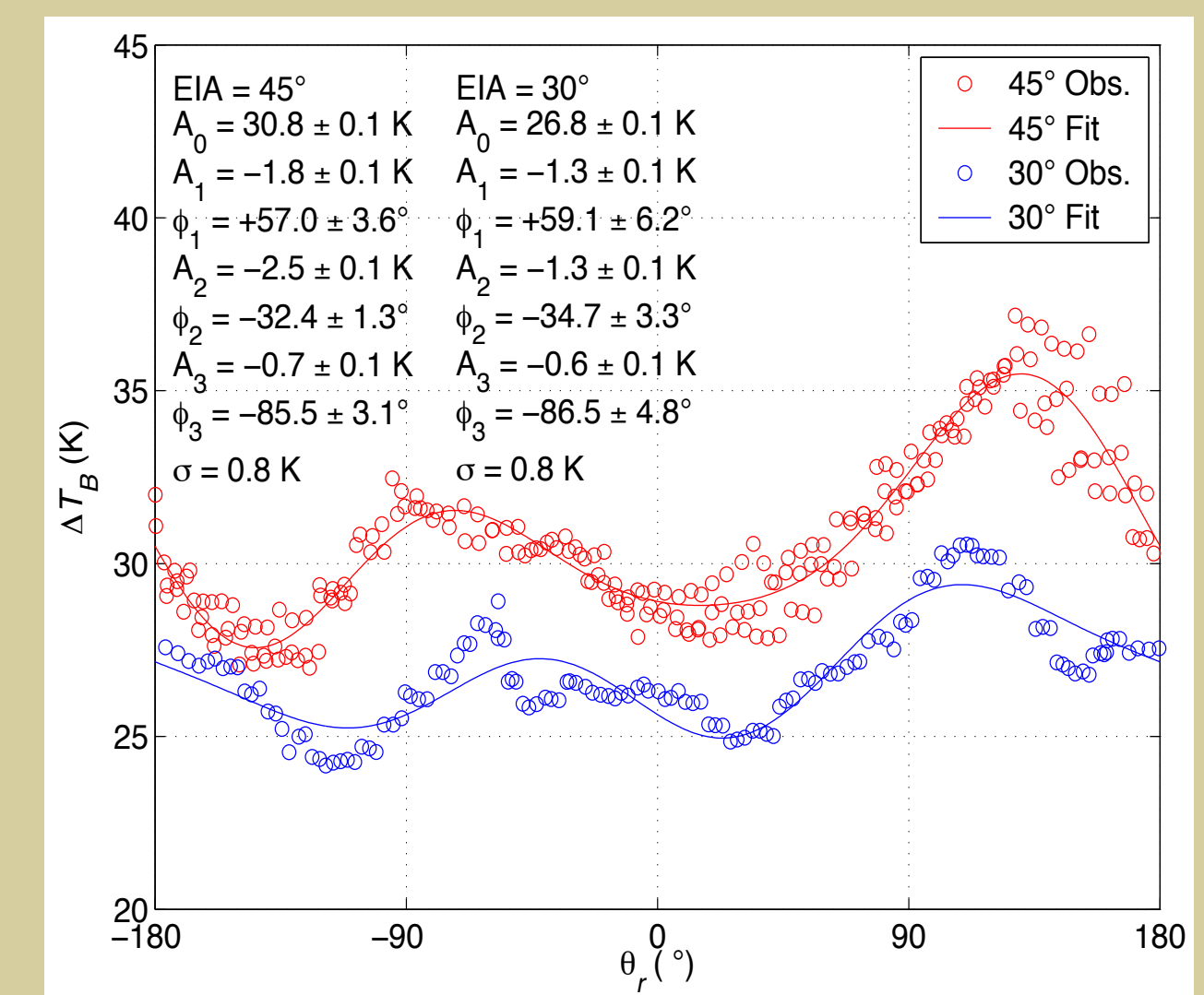


Figure 6: Example Fourier fits to observed ΔT_B at 5.31 GHz plotted as a function of θ_r for 30° and 45° incidence angles.

5. Findings From Gustav

- The mean (A_0) ΔT_B is quantitatively similar to that found at nadir.
- A double-harmonic oscillation is evident in the ΔT_B measurements.
- The first harmonic term (A_1) has been interpreted as a difference in upwind vs. downwind T_B (Kunkee and Gasiewski, 1997).
- The second harmonic term (A_2) is attributed to an asymmetry caused by the distribution of foam on longer waves.

6. WindSat

- Due to a lack of SFMR measurements to confirm the findings from Gustav, WindSat T_B measurements are analyzed to determine if a similar signal can be found.
- The spaceborne WindSat polarimetric radiometer has 5 channels, one of which is 6.8 GHz (Gaiser et al. 2004).
 - The 6.8 GHz channel measures at an EIA of 53.5° with a horizontal spatial resolution of 39 X 71 km.
- For WindSat, the T_B measurements are plotted as a function of θ_r where the relative azimuth angle used for WindSat is the compass azimuth angle (Figure 7).

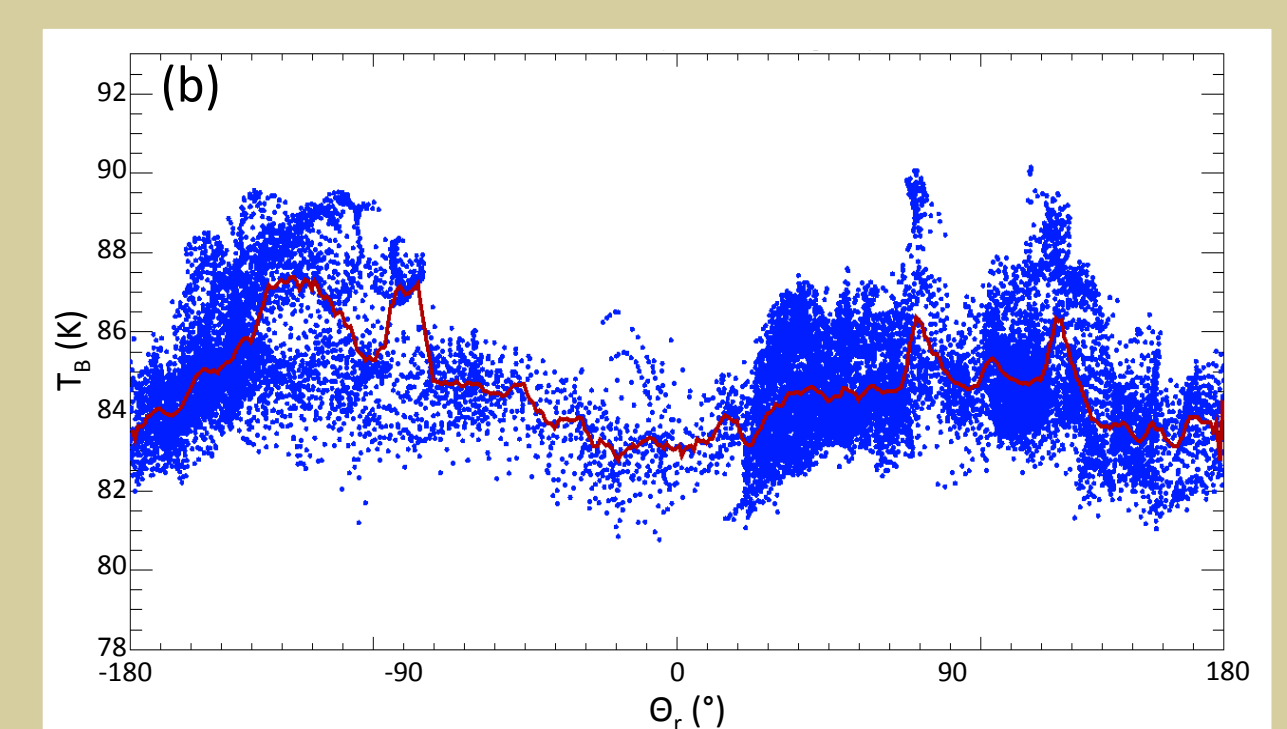
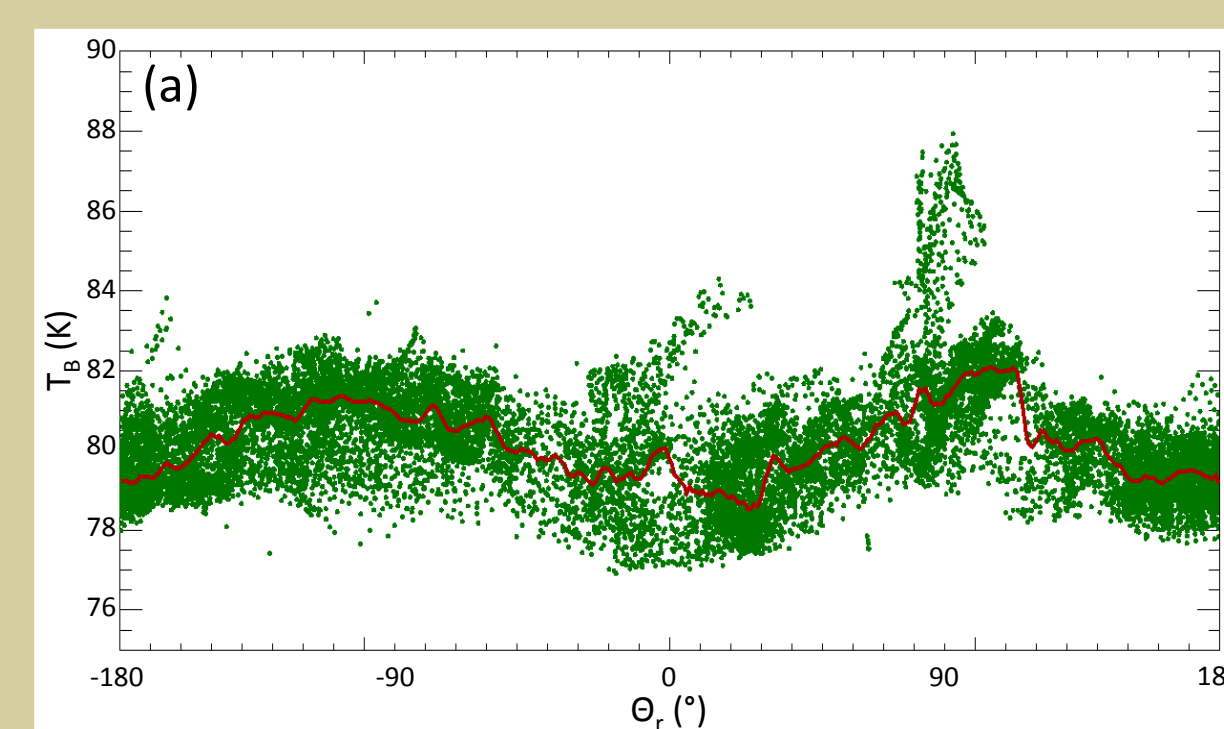


Figure 7: Example plots of WindSat T_B versus θ_r for wind speed bins of 12–14 m/s (a) and 16–18 m/s (b). The red line indicates a running mean of the median T_B for 1° θ_r bins.

- A similar signal to that found in the SFMR data is seen for T_B measurements at wind speeds of 12–22 m/s.
 - More data is needed to confirm a signal at higher wind speeds.

7. Future Work

- More SFMR measurements will be obtained during the upcoming North Atlantic hurricane season to confirm the results from Gustav.
- Wave data from the Scanning Radar Altimeter (SRA) will be collected.
- Further analysis of WindSat T_B data will be completed to determine the wind and wave direction influence on the retrievals.
- Wave impacts will be analyzed using WaveWatch III (Tolman 2002).
- Relationships found could potentially be applied to the Hurricane Imaging Radiometer (HIRad), which was designed based on the SFMR to provide a swath of measurements over EIA of $\pm 60^\circ$.

9. Acknowledgements

We thank NASA OVVST for funding this research and the pilots and crew at NOAA/Aircraft Operations Center.